



Article

# Assessment of Fibrinogen Thermal Conductivity and Interaction Energy with Polyarylethersulfone (PAES) Clinical Hemodialysis Membranes at Normal and Elevated Patient Body Temperatures

Arash Mollahosseini<sup>1</sup> and Amira Abdelrasoul<sup>1,2,\*</sup> 

<sup>1</sup> Department of Chemical and Biological Engineering, University of Saskatchewan, 57 Campus Drive, Saskatoon, SK S7N 5A9, Canada

<sup>2</sup> Division of Biomedical Engineering, University of Saskatchewan, 57 Campus Drive, Saskatoon, SK S7N 5A9, Canada

\* Correspondence: amira.abdelrasoul@usask.ca; Tel.: +(306)-966-2946; Fax: +(306)-966-4777

**Abstract:** Fibrinogen (FB) can trigger several biological reactions and is one of the critical proteins targeted during hemodialysis (HD). A better understanding of the thermal behavior of FB and its interactions with polymeric membranes during the HD process is needed in both normal and fever temperature conditions. This study calculated the thermal behavior of FB along with its interaction energy with polyarylethersulfone (PAES) clinical HD membranes using molecular dynamics (MD) approaches. The Dreiding force field was used for the MD simulations. The influence of temperature on the thermal conductivity (TC) and the interaction energy of the FB structure was assessed to understand the activation trends in fever conditions. Based on the MD simulation, the TC of FB at normal body temperature was 0.044 and 0.084 W/m·K according to equilibrium and non-equilibrium approaches, respectively. The elevation of temperature from normal to fever conditions increased the thermal conduction of FB to 0.577 and 0.114 W/m·K for equilibrium and non-equilibrium approaches, respectively. In addition, the elevation of patient blood temperature resulted in nearly 32 kcal/mol higher total interaction energy between FB and the PAES model. When end-stage renal disease (ESRD) patients have a HD session and experience fever and elevated temperature as a side effect, the interaction between FB and the membrane increases. More importantly, FB is exposed to more heat passage and accordingly more temperature-induced confirmation and activation compared to other human serum proteins such as albumin.

**Keywords:** hemodialysis; membrane; human serum fibrinogen; thermal conductivity; interaction energy



**Citation:** Mollahosseini, A.; Abdelrasoul, A. Assessment of Fibrinogen Thermal Conductivity and Interaction Energy with Polyarylethersulfone (PAES) Clinical Hemodialysis Membranes at Normal and Elevated Patient Body Temperatures. *C* **2023**, *9*, 33. <https://doi.org/10.3390/c9010033>

Academic Editor: Giuseppe Cirillo

Received: 26 December 2022

Revised: 6 March 2023

Accepted: 8 March 2023

Published: 12 March 2023



**Copyright:** © 2023 by the authors. Licensee MDPI, Basel, Switzerland. This article is an open access article distributed under the terms and conditions of the Creative Commons Attribution (CC BY) license (<https://creativecommons.org/licenses/by/4.0/>).

## 1. Introduction

Hemodialysis (HD) is a life-sustaining treatment for end-stage renal disease (ESRD) patients. Despite the ability of the HD process to remove metabolites, high mortality and morbidity rates are still reported [1]. Many side effects or complications can occur, including inflammation (due to interactions between human serum proteins (HSPs) and HD membranes) and cardiovascular complications due to protein attachment to the HD membrane surface [2–5]. Interactions, protein adsorption, and fouling, which contribute to cardiovascular shocks, are responsible for more than half of the mortality rate. The interactions and protein conformation changes that activate the immune system and other cascades in the body are the result of the incompatibility of HD membranes with the patient's blood (lack of hemocompatibility) [6–8]. Despite several advances in the field, knowledge of these interactions is still limited.

Computational studies and molecular dynamics (MD) simulations in particular have been increasingly employed in recent decades in the field of materials science and membrane technology [9]. Computational frameworks have also seen significant use for medical

and biomedical engineering purposes [10–12]. MD efforts aid research in these areas by either predicting the behavior of the materials or calculating their properties at the molecular level [13–16]. Despite the advantages of MD frameworks for materials science and membrane technology, their application in HD membrane assessment has only recently been reported. Sasongko et al. report molecular docking of urea and creatinine uremic toxins in the polymeric structure of polysulfone (PSF) [17]. Our recent publication reveals the unique application of MD frameworks for HD membrane interactions with HSPs, simplified water interaction simulations with membranes, and the experimental assessment of the interaction [18,19]. The frameworks introduced also apply to membrane separation processes beyond HD [20,21]. Recent MD efforts in the area of membrane separation and porous media and recent insights related to dialysis are reviewed by the same authors [22,23].

Understanding the behavior of the HSPs is important for medical science and biomedical engineering applications because several vital biological functions are carried out by these proteins in the human body. Folding of these proteins can result in their malfunction and related diseases [24]. Understanding the folding and misfolding of the proteins is crucial as this can lead to the formation of amyloids and cardiovascular shocks [25]. Several phenomena can contribute to the folding of proteins. Common reasons for protein denaturation as previously described by Mollahosseini et al. include altering the chemical balance in the blood (pH change), mechanical shocks (attachment of proteins to a foreign surface), and temperature-induced shocks (fever). Figure 1 is a schematic of these denaturation pathways. Measuring the characteristics of the proteins can be challenging due to their small size and limitations related to experimental instrumentation and technical approaches, so computational approaches can be helpful in this regard. The thermal conductivity (TC) of proteins is important as it reflects the capacity of the biological structure to conduct (expose itself to) heat. Accordingly, understanding the TC profile of a protein structure can be important for better explaining folding and aggregation behavior.

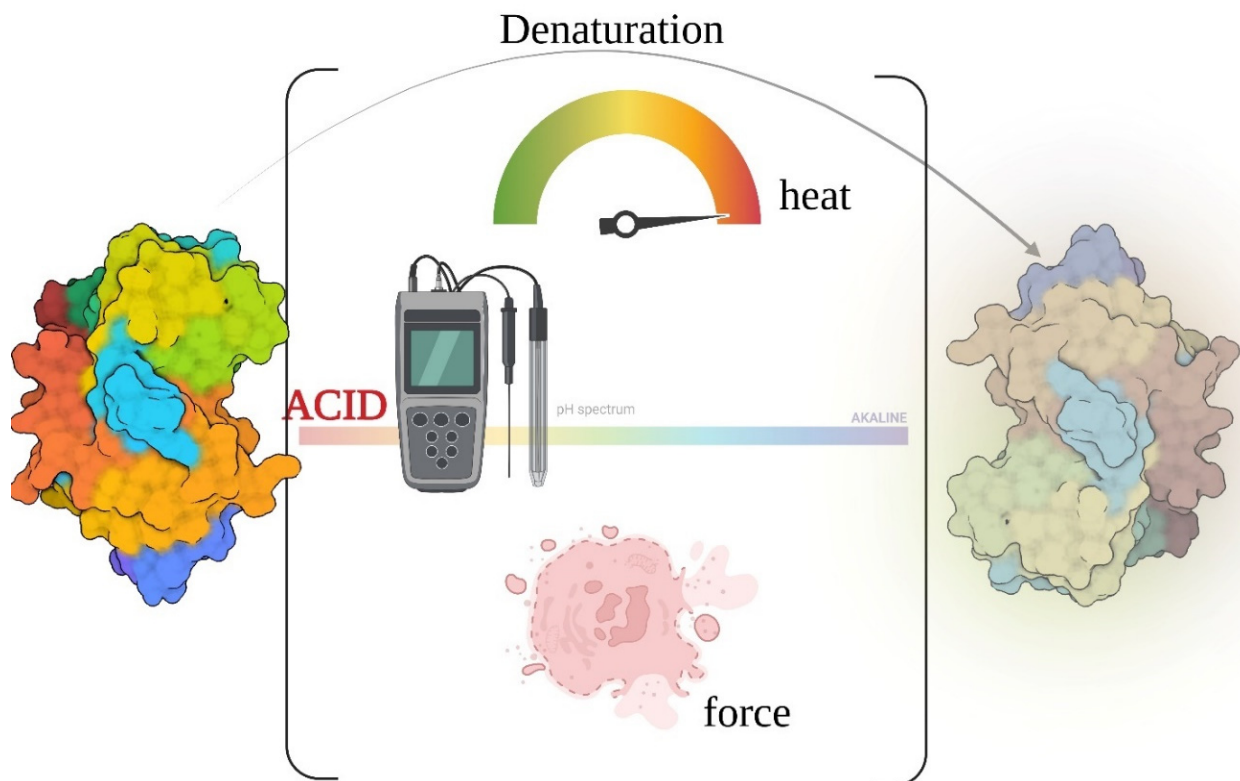


**Figure 1.** Denaturation of blood proteins with changes in temperature, environmental pH, and mechanical shocks [23] (with permission from Elsevier).

Among the HSPs, the thermal behavior of human serum albumin (HSA) has been calculated using MD tools [26]. HSA's TC will drop with an increase in temperature and accordingly this protein is exposed to less heat transfer and denaturation. Another HSP, fibrogenin (FB), is reported in high concentrations in the blood of kidney failure patients [27]. FB contributes to the coagulation cascade [28] and, accordingly, can facilitate the adhesion and aggregation of platelets on an external surface when it contacts blood [6,29]. Elevation FB levels are associated with cardiovascular risks [30,31] a non-linear relationship between the FB content in dialysis patient blood and cardiovascular shock-assisted mortality has been reported [32]. Heat can promote the folding of FB, so assessing the TC of the FB and its correlation with elevated temperature, i.e., during fever (a side effect of dialysis), is important. As such, this study focuses on assessing the TC of FB (Figure 2) as one of the most important proteins in the bloodstream interacting with the HD membrane.

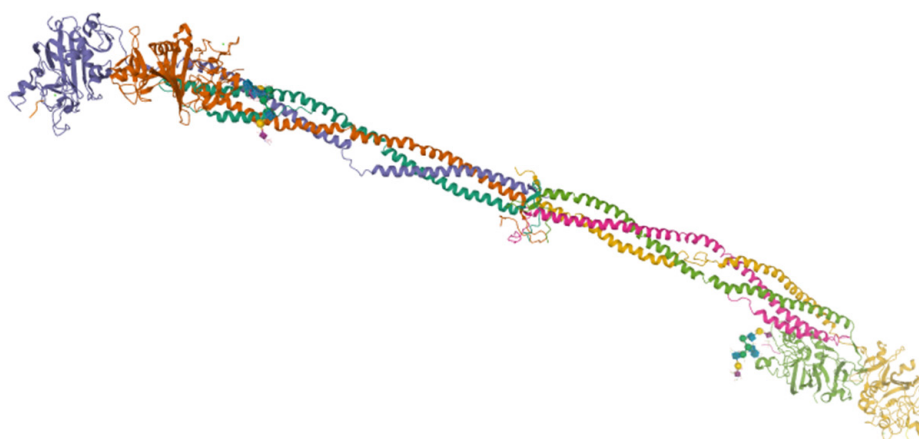


**Figure 2.** Schematic structure of fibrinogen.

There are previous reported efforts of the measurement of proteins' thermal conductivity, experimentally. An instance of these approaches could be the measurement of energy transport through a solution of  $\alpha$ -aminoisobutyric acid-based structures in chloroform [33]. The study reported the thermal conductivity measured non-equilibrium molecular dynamics computational measurement as well. While the experimental approaches could offer a realistic value, several parameters such as experimental errors, interference of structures and solvents on each other, etc., might affect the final result. On the other hand, computational studies could focus on one single protein structure and avoid interference effects. MD approaches are also used for the calculation of the thermal conductivity of various proteins such as villin headpiece subdomain [34], 7S globulin [35], 11S globulin [36], and natural silk structure [37].

Computational efforts to better understand the thermal behavior of FB, along with many other essential blood proteins, in the HD process have not been reported. Accordingly, the objectives of this study were to: (i) calculate the TC of FB using previously established MD frameworks; (ii) investigate the influence of elevated temperature (resembling fever conditions in patients) on the TC of FB; (iii) measure the binding energy of FB to aryl sulfone HD membranes; and (iv) compare the binding energies for normal and fever condition temperatures.

## 2. Computational Methods

The atomic interactions of the structures of both FB and membrane oligomers were defined using the Dreiding force field potential, which is appropriate for biological, organic, and main group inorganic structures [38]. The Dreiding force field is a generic potential and therefore can be used to simulate both biological protein structures and organic polymeric chains. This force field has been used to calculate the TC of different proteins and for interaction energy calculations [18,26]. The cut-off for non-bond

interactions was considered to be 10 Å. The FB structure was obtained from the protein databank (PDB ID 3GHG). The structure of FB, details regarding its active sites, the PDB-ID and its root mean square distance, and amino acid active sites are described in our previous publication [18]. Visual molecular dynamics (VMD) software was used for visualization purposes [39]. The polymeric chains were built and minimized using Avogadro software [40]. Packing polymeric chains to create a membrane model and creating a simulation box with membranes and proteins were accomplished using PACKMOL software [41]. Polyarylethersulfone (PAES) (Figure 3) was chosen as the membrane material as it is commonly used in Canadian hospitals [18]. Polymeric chains were built by attaching five monomers of PAES using Avogadro. Membranes were built by packing 70 polymer chains in a slab with dimensions of 300 Å × 300 Å × 30 Å. The authors tried creating membranes with a higher number of polymeric chains; however, this resulted in either the failure of the PACKMOL software to fit the chains in the box or a long simulation time during the data generation process. Validation of the simulated polymer was performed using a density calculation (consecutive NPT ensemble; 500 ps NPT run at 1 bar, 100 ps run at 100 bar, 100 ps run at 10,000 bar, and final value after 500 ps run at 1 bar) [18]. The calculated equilibrium density of PAES was 1.22 g/cm<sup>3</sup>, which is close to the actual density of 1.37 g/cm<sup>3</sup> [42].

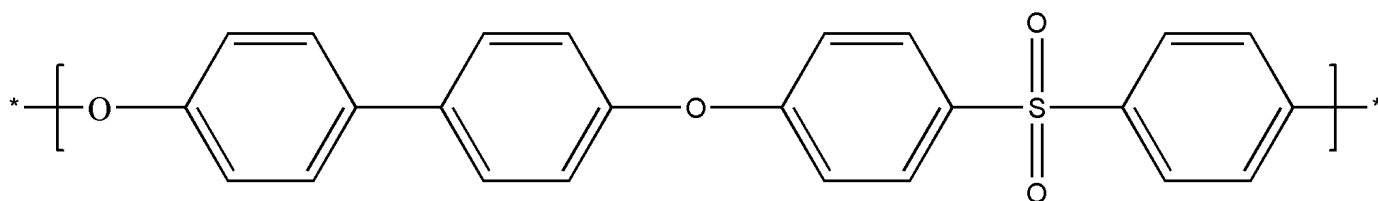


**Figure 3.** Polyarylethersulfone structure.

Interaction simulations were conducted as follows. The FB was initially located on the top of the membrane model at a distance of 100 Å. The simulation was performed for 1000 steps. Then, the protein was moved to the surface of the membrane model so it could interact with the polymeric structure. The simulation proceeded again for another 1,000,000 steps. The protein was then moved away from the polymer structure, and the simulation was run for another 10,000 steps. The boundary conditions were set to be periodic. The MD simulations were conducted at 298 K, 310.15 K (normal body temperature), and 311.65 K (representing fever temperature) using the Langevin thermostat ensemble. The NVE ensemble was used prior to the Langevin thermostat for the equilibrium process. The energy term calculated in the simulation is the total interaction energy imposed by the macromolecule protein to the polymeric structure. The binding interaction energy was also calculated by subtracting the total energy of the FB and the polymeric structure from protein + polymer energy [22]. To eliminate any interference due to the environment, the interaction simulations were performed with only polymer and FB structures without the further addition of water or air molecules, similar to the authors' previous publications [18,21,43].

The TC was measured using equilibrium MD (EMD) and non-equilibrium MD (NEMD) approaches [26]. TC simulations were performed for 1 ns. The FB structure was located in the center of a box with water molecules used to fill the void areas and hydrate the box. The TC was computed using the Green-Kubo theory and the NVE ensemble. The Fourier theory was also implemented for TC calculations via NEMD simulation. In this simulation, by applying NVT and then NVE ensembles, the TC of the hydrated FB was measured after a 1 ns simulation. Water molecules were simulated using the TIP3P model.

The simulations here were not repeated in this research. The authors have previously reported the reliability of the methods used for interaction energy studies in their previous articles [18,19,21]. The interaction studies between modeled membranes and human serum protein approaching interacting with the membrane by different angles were also reported in the same teams' previously published article [43]. The thermal conductivity measure-

ments were not repeated as the previous computational-based published papers which measured thermal conductivity did not repeat the simulations for reliability purposes [26].

### 3. Results and Discussion

#### 3.1. Thermal Conductivity

Stabilization of the system prior to TC calculation was performed using an NPT ensemble for both non-equilibrium and equilibrium calculations. The NVT ensemble was used along with the well-known Green–Kubo method according to the following equation:

$$k = \frac{1}{3k_B VT^2} \int_0^\infty \langle S(t) \cdot S(0) \rangle dt \quad (1)$$

where  $K$  is the TC,  $T$  is the temperature,  $S$  is the heat flux,  $V$  represents the simulated volume, and  $K_B$  denotes the Boltzmann constant. The normalized heat flux and TC are reported for hydrated FB boxes at different temperatures.

The Furrier equation was used to calculate the equilibrium TC of hydrated FB located between a heat source and heat sink (high and low-temperature sources, respectively):

$$k = \frac{\frac{dQ}{dt}}{A \left( \frac{dT}{dx_1} + \frac{dT}{dx_2} \right)} \quad (2)$$

where  $\frac{dQ}{dt}$  is the heat variations through time,  $A$  is the surface area of the box, and  $\frac{dT}{dx_1}$  and  $\frac{dT}{dx_2}$  are the temperature gradient of the hot and cold sources, respectively. Different values calculated for the TC are reported in Table 1.

**Table 1.** Thermal conductivity of FB at normal and fever temperatures.

Temperature (K)	EMD (W/m·K)	NEMD (W/m·K)
310.15	0.044	0.084
311.65	0.577	0.114

The TC of the FB at normal body temperature was determined to be 0.04 W/m·K using the EMD and 0.08 W/m·K using the NEMD approaches. An elevation of TC values was observed after increasing the temperature. The TC is a function of the nanoscale structure; specifically, the parameter is a function of temperature, crystallinity of the protein, molecular chain alignment, and chemical bonding.

#### 3.2. Interaction Studies

An elevated temperature could increase the resonance of atoms, which could consequently result in the limitation of the effective movements of the structures and reduction in the TC [26]. A similar study targeted HSA and demonstrated the influence of the protein's number on the value of the TC [26]. The thermal conductivity for the HSA was reported to be equal to 0.496, 0.491, and 0.483 W/m·K for the simulations with one, two, and three protein structures, respectively. A decrease in the TC of biological structures with increasing temperature has also been reported for DNA structures [44]. The TC of blood constituents and biological structures of the human body is reported to be less than that of water (0.598 W/m·K) [26,44,45]. An increase in the biological content of the simulation cell could push the final TC to values less than the TC of water. As reported in the previous section, the TC of FB is less than that of water, which lends credibility to the current study. The TC of FB at normal body temperature was estimated to be 0.08 and 0.04 W/m·K using NEMD and EMD approaches, respectively. At fever conditions (elevated temperature), these values were 0.11 and 0.58 W/m·K, respectively. The levels of FB are reportedly high in HD patients [46–49]. When these patients experience fever (along with exposure of their blood to HD membranes with poor compatibility), some serum proteins such as



FB could be affected. While previous computational reports show HSA's TC decreases with an increase in temperature, the present study indicates FB experiences an opposite effect [26]. This could result in higher heat passage through FB in comparison with other proteins, consequently resulting in thermal-induced conformation change and activation. Accordingly, the different thermal behavior of FB is one possible explanation for its higher concentration in CKD patients.

The total energy was assessed in simulations in which FB and PAES were interacting at different temperatures. Figure 4 reflects the total interaction energies for FB in the vicinity of the PAES membrane. Table 2 summarizes the energy values resulting from FB-PAES simulations. This method has been used along with experimental frameworks by the same authorship for common HSPs (HSA, FB, and human serum transferrin (TRF)) [18]. Nonbond interactions can alter the interaction pattern between blood proteins and blood filtration membranes [50]. This interactive pattern could initially control the provocation of the proteins, which consequently results in the inactivation of the proteins and compatibility issues for the incorporated membrane.

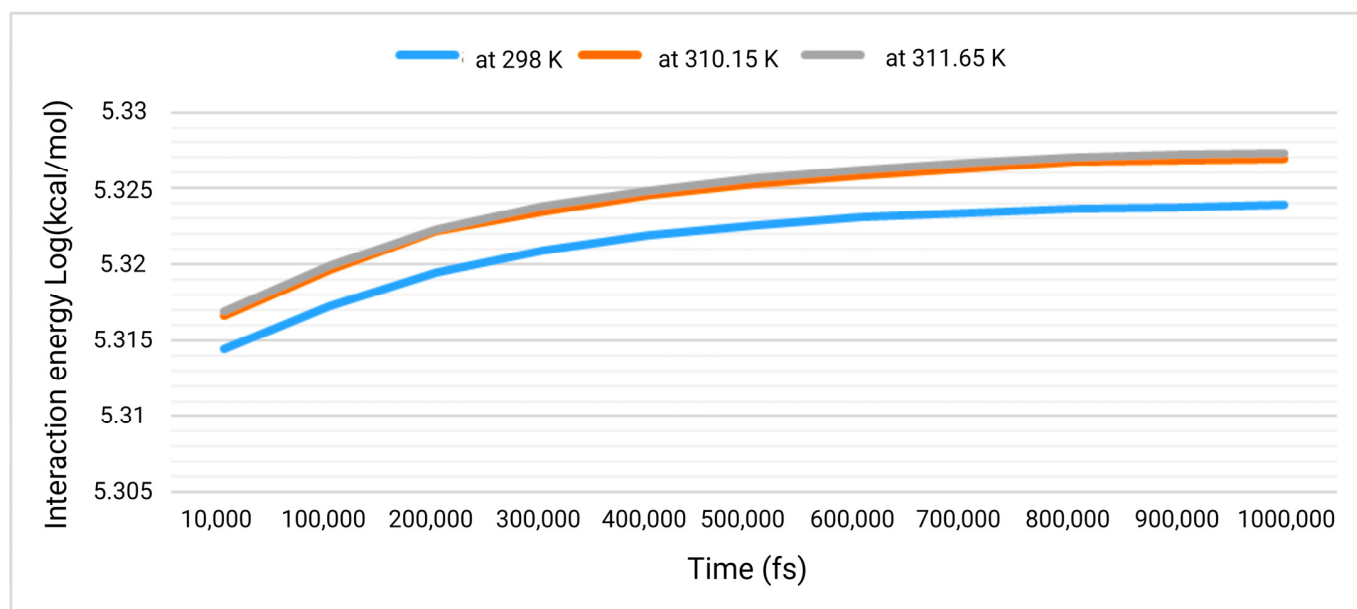


**Figure 4.** Total energy trend between FB and PAES membrane model.

**Table 2.** Interaction energies between FB and the aryl sulfone membrane.

Polymer-Protein Interaction	Total Energy (kcal/mol)	van der Waals Interaction (kcal/mol)	Electrostatic Interaction (kcal/mol)	Hydrogen Bonding (kcal/mol)	Number of Hydrogen Bonds	Binding Energy (kcal/mol)
T1-PAES-FB *	231,664.31	16,233.86	36,347.13	−192.24	1306	52,383.50
T2-PAES-FB *	233,075.42	16,392.48	36,269.15	−189.33	1305	52,318.88
T3-PAES-FB *	233,107.8	16,370.63	36,218.66	−188.28	1306	52,167.98

\* T1 = 298 K, T2 = 310.15, T3 = 311.65.

As depicted in Figure 4, the interaction energy values start to increase and reach a stable value after the 900,000th step. Based on the values reported in Table 2, the interaction energy increases by 32 kcal/mol when body temperature increases from normal (310.16 K) to fever (311.65 K) conditions. Figure 5 is a schematic of the MD scenario as well as the MD capture of the simulation performed. Figure 6 reflects the binding energy between the protein and the polymeric membrane model. Assessment of the binding interaction energy shows a decrease concurrent with the increase in temperature. Increasing the temperature from room temperature to body temperature results in a decrease in the binding energy of 64.62 kcal/mol (from 52,383.50 to 52,318.88 kcal/mol). A further

change in the temperature from body temperature to fever conditions results in a further 150.9 kcal/mol decrease in the binding energy (from 52,318.88 to 52,167.98 kcal/mol).

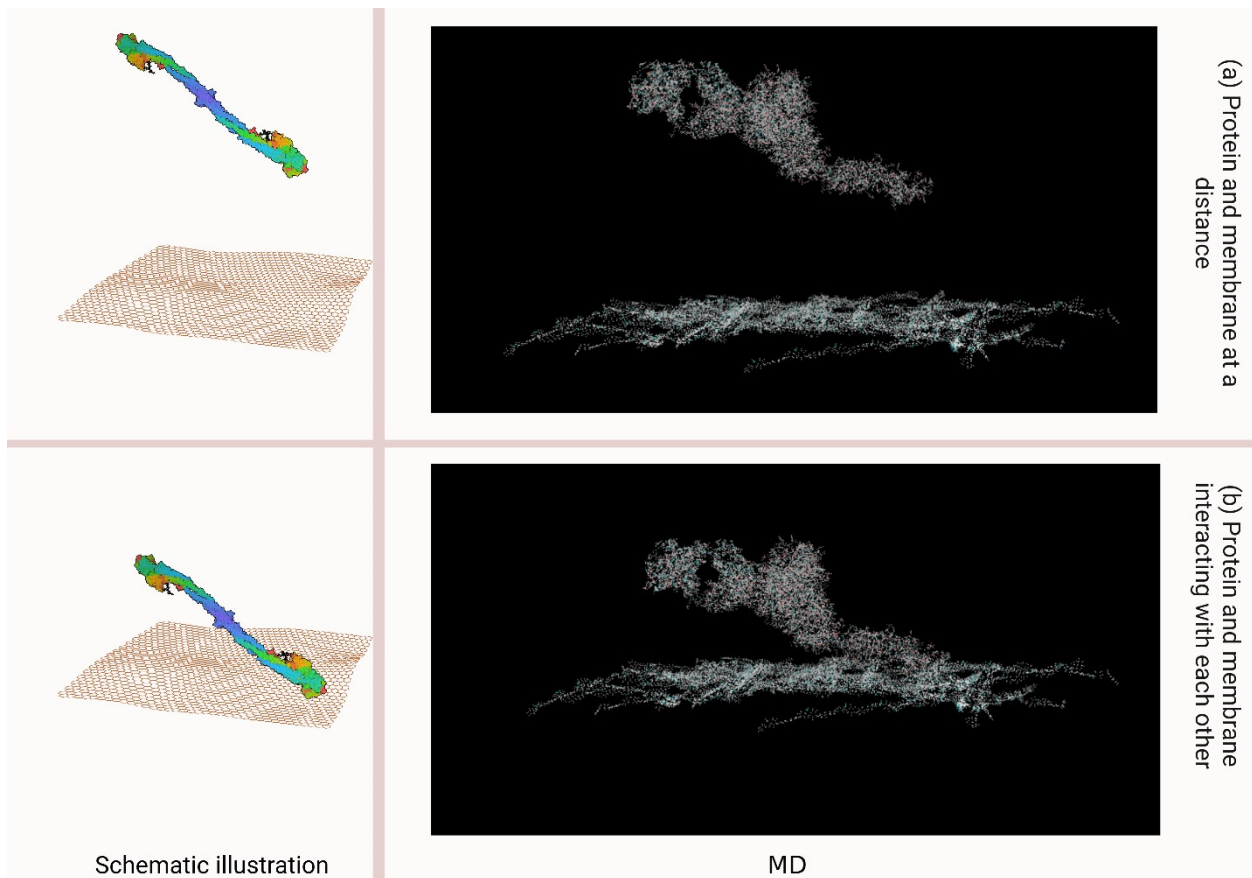


**Figure 5.** Schematic illustration (left) and MD capture (right) of the fibrinogen and polymeric membrane model (a) far from each other and (b) interacting with each other.

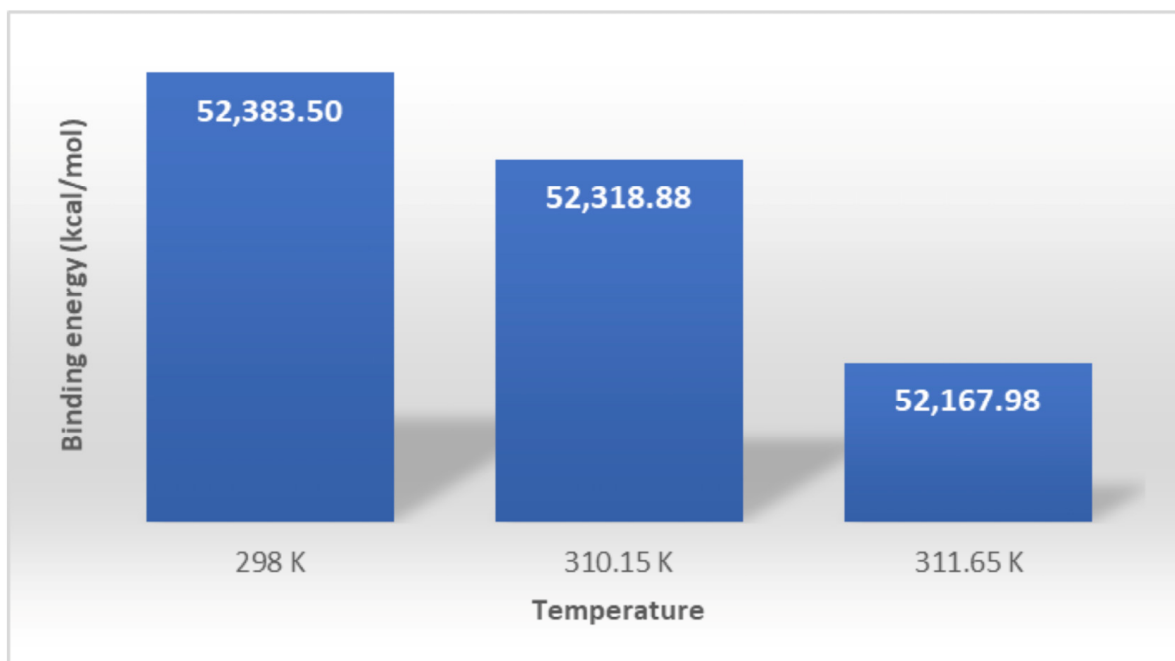


**Figure 6.** Binding energy of fibrinogen and PAES polymeric membrane model at different temperatures.

A closer look at the trends of each type of energy shows an increasing trend in van der Waals (VDW) energy from 298 to 310.15 K. However, electrostatic interactions decrease when the temperature is elevated from 298 K to 310.15 K, and further decrease with fever temperature. This could be interpreted as the higher contribution of VDW energy to the overall interaction energy in comparison with electrostatic energies resulting from charged moieties on both the membrane and protein structures. The higher contribution of VDW energy was observed in a previous study [18].

Hydrogen bonding is another aspect that could affect the interaction and binding energy trends. For smaller chemical structures such as urea and creatinine, or for solutes studied in aqueous media filtrations, higher hydrogen bonding (between the polymeric film and the solute) is interpreted as a higher capability of the solute to pass through the membrane [51–53]. Previous studies by the same group also show HSA and TRF can be more prone to attachment to the surface as they possess a higher number of weak hydrogen bonds (which could manipulate the interfacial adhesion) [54]. As reported in Table 2, increasing the temperature from normal body temperature to fever temperature results in lower intensities and a higher number of hydrogen bonds. Accordingly, fever temperature could elevate the level of FB activation on the membrane surface.

Reversible or irreversible deactivation and denaturation of the native structure of proteins can occur as a result of high pressure, chemical imbalance, high acidity, and high temperature. Molecular mechanisms of the denaturation and unfolding are different in each aforesaid scenario [55]. Heat exposure can result in aggregation and gel formation (coagulation) of proteins if the concentration is sufficiently high [56]. Considering the separation mechanisms of HD membranes (molecular sieving and diffusion, or convective mass transfer), the concentration of proteins will increase on the surface of the membrane when uremic metabolites and extra water are removed. In addition to incompatibility of the membrane with the blood, temperature increase due to possible shocks and fevers in ESRD patients could increase the chances of coagulation-mediated activation of the proteins and, consequently, their fouling on the dialysis membrane. While some proteins such as HSA will show a decrease in TC with higher temperature (which could be due to a natural defense system that prohibits the protein from excessive folding), FB will allow higher heat passage through its structure.

Most biological structures have a high water content, so calculated TCs are expected to be near  $0.6 \text{ W/m}\cdot\text{K}$ . The computationally calculated TC of blood proteins is reported to be near  $0.5 \text{ W/m}\cdot\text{K}$  [26]. Computational-driven values are always a function of the force fields, assumptions, simplifications, and simulation setups. Our calculations determined a similar value for FB in the EMD simulation scenario at the higher temperature; however, the increasing trend of the TC value with temperature is more interesting as it gives insights regarding the behavior of FB in fever conditions. The higher total energy is mainly due to the increased movement of atoms within the molecular structure. The decrease in binding energy shows that FB could have less tendency to foul on the membrane at fever temperature.

#### 4. Conclusions

Computational studies are becoming more and more common in the area of chemical and materials engineering with a coincident better understanding of the issues with various computational tools. Knowledge regarding how simulation and modeling procedures are different could result in better comprehension of the results and their differences. Some differences in simulation approaches can result in different final values that cannot be compared with other published data. Creating a realistic environment, such as with a high number of water molecules in the simulation, could generate a more accurate final result, especially when thermodynamic characteristics are being discussed [26,36]; however, this can also result in interference with the interactions and long computation times. System sampling is another important factor. The bigger the biomolecules, the more challenging it becomes to reach a realistic final result because more angles, functional groups, or active



sites must be considered. Parameters such as surface energy of interacting materials, buffer pH, temperature, and time might also lead to incompatible numerical results from study to study [57]. This could happen in computational areas as well.

A computational framework using MD simulations was incorporated in this study to simultaneously measure the temperature-dependent interactions between FB and aryl sulfone membrane models and the TC of the FB structure. MD studies were performed to better understand the effect of elevated temperature during fever side effects experienced by HD patients on the interaction of their blood with the HD membrane material. Based on the MD results, the TC of the FB was calculated to be 0.044 W/m·K based on an equilibrium approach. Temperature elevation resulted in an increase in the TC, which can be interpreted as more exposure of the protein to heat flux. Temperature elevation from normal to fever conditions led to a nearly 32 kcal/mol increase in total interaction energy. Findings from this study, informed by those of other computational studies, suggest fever side-effects in HD patients could result in FB temperature-induced activation and could be one reason why HD patients have an elevated level of FB in their bloodstream.

**Author Contributions:** A.A. incepted the hemodialysis (HD) membranes research program in Canada, conceived the study design and the research methodology, and was in charge of overall direction and planning; A.M. performed the computational study and its analyses under the supervision of A.A.; A.A. prepared the final manuscript and oversaw its revisions. All authors have read and agreed to the published version of the manuscript.

**Funding:** The authors would like to acknowledge and express their gratitude to the Natural Sciences and Engineering Research Council (NSERC)—Discovery Grant (DG) for funding the research and to the Chemical and Biological Engineering Department at the University of Saskatchewan for the support provided.

**Data Availability Statement:** The raw/processed data required to reproduce the findings of this study are available from the corresponding author [Amira Abdelrasoul] upon reasonable request.

**Code Availability:** The code to reproduce these findings cannot be shared at this time, as the data is critical to the ongoing research.

**Conflicts of Interest:** The authors have no relevant financial or non-financial interests to disclose.

## Abbreviations

Name	Acronyms
Chronic kidney disease	CKD
End-stage renal disease	ESRD
Fibrinogen	FB
Hemodialysis	HD
Human serum albumin	HSA
Human serum protein	HSP
Human serum transferrin	TRF
Molecular dynamics simulation	MD
Polyarylethersulfone	PAES
Polysulfone	PSF
Thermal conductivity	TC
van der Waals	VDW

## References

1. Choi, S.R.; Lee, Y.-K.; Cho, A.J.; Park, H.C.; Han, C.H.; Choi, M.-J.; Koo, J.-R.; Yoon, J.-W.; Noh, J.W. Malnutrition, inflammation, progression of vascular calcification and survival: Inter-relationships in hemodialysis patients. *PLoS ONE* **2019**, *14*, e0216415. [[CrossRef](#)] [[PubMed](#)]
2. Tong, J.; Liu, M.; Li, H.; Luo, Z.; Zhong, X.; Huang, J.; Liu, R.; He, F.; Fu, J. Mortality and associated risk factors in dialysis patients with cardiovascular disease. *Kidney Blood Press. Res.* **2016**, *41*, 479–487. [[CrossRef](#)]
3. Sarnak, M.J. Cardiovascular complications in chronic kidney disease. *Am. J. Kidney Dis.* **2003**, *41*, 11–17. [[CrossRef](#)]

4. Inrig, J.K. Intradialytic hypertension: A less-recognized cardiovascular complication of hemodialysis. *Am. J. Kidney Dis.* **2010**, *55*, 580–589. [[CrossRef](#)]
5. Thomas, R.; Kanso, A.; Sedor, J. Chronic kidney disease and its complications. *Prim. Care Clin. Off. Pract.* **2008**, *35*, 329–344. [[CrossRef](#)] [[PubMed](#)]
6. Mollahosseini, A.; Abdelrasoul, A.; Shoker, A. A critical review of recent advances in hemodialysis membranes hemocompatibility and guidelines for future development. *Mater. Chem. Phys.* **2020**, *248*, 122911. [[CrossRef](#)]
7. Mollahosseini, A.; Abdelrasoul, A.; Shoker, A. Challenges and advances in hemodialysis membranes. *Adv. Membr. Technol.* **2020**, *151*.
8. Mollahosseini, A.; Abdelrasoul, A.; Shoker, A. Latest advances in zwitterionic structures modified dialysis membranes. *Mater. Today Chem.* **2020**, *15*, 100227. [[CrossRef](#)]
9. Khoshhal Salestan, S.; Seyedpour, S.F.; Rahimpour, A.; Shamsabadi, A.A.; Tiraferri, A.; Soroush, M. Molecular Dynamics Insights into the Structural and Water Transport Properties of a Forward Osmosis Polyamide Thin Film Nanocomposite Membrane Modified with Graphene Quantum Dots. *Ind. Eng. Chem. Res.* **2020**, *59*, 14447–14457. [[CrossRef](#)]
10. Karimipour, A.; Karimipour, A.; Jolfaei, N.A.; Hekmatifar, M.; Toghraie, D.; Sabetvand, R.; Rostami, S. Prediction of the interaction between HIV viruses and human serum albumin (HSA) molecules using an equilibrium dynamics simulation program for application in bio medical science. *J. Mol. Liq.* **2020**, *318*, 113989. [[CrossRef](#)]
11. Durrant, J.D.; McCammon, J.A. Molecular dynamics simulations and drug discovery. *BMC Biol.* **2011**, *9*, 71. [[CrossRef](#)] [[PubMed](#)]
12. Lemkul, J.A.; Bevan, D.R. Assessing the stability of Alzheimer’s amyloid protofibrils using molecular dynamics. *J. Phys. Chem. B* **2010**, *114*, 1652–1660. [[CrossRef](#)] [[PubMed](#)]
13. Noorian, H.; Toghraie, D.; Azimian, A. The effects of surface roughness geometry of flow undergoing Poiseuille flow by molecular dynamics simulation. *Heat Mass Transf.* **2014**, *50*, 95–104. [[CrossRef](#)]
14. Toghraie, D.; Mokhtari, M.; Afrand, M. Molecular dynamic simulation of copper and platinum nanoparticles Poiseuille flow in a nanochannels. *Phys. E Low-Dimens. Syst. Nanostructures* **2016**, *84*, 152–161. [[CrossRef](#)]
15. Afrouzi, H.H.; Ahmadian, M.; Moshfegh, A.; Toghraie, D.; Javadzadegan, A. Statistical analysis of pulsating non-Newtonian flow in a corrugated channel using Lattice-Boltzmann method. *Phys. A Stat. Mech. Its Appl.* **2019**, *535*, 122486. [[CrossRef](#)]
16. Alrashed, A.A.; Akbari, O.A.; Heydari, A.; Toghraie, D.; Zarringhalam, M.; Shabani, G.A.S.; Seifi, A.R.; Goodarzi, M. The numerical modeling of water/FMWCNT nanofluid flow and heat transfer in a backward-facing contracting channel. *Phys. B Condens. Matter* **2018**, *537*, 176–183. [[CrossRef](#)]
17. Sasongko, N.; Siahaan, P.; Lusiana, R.A.; Prasasty, V. Understanding the interaction of polysulfone with urea and creatinine at the molecular level and its application for hemodialysis membrane. In *Journal of Physics: Conference Series*; IOP Publishing: Bristol, UK, 2020.
18. Mollahosseini, A.; Argumeedi, S.; Abdelrasoul, A.; Shoker, A. A case study of poly (aryl ether sulfone) hemodialysis membrane interactions with human blood: Molecular dynamics simulation and experimental analyses. *Comput. Methods Programs Biomed.* **2020**, *197*, 105742. [[CrossRef](#)]
19. Mollahosseini, A.; Saadati, S.; Abdelrasoul, A. Effects of mussel-inspired co-deposition of 2-hydroxymethyl methacrylate and poly (2-methoxyethyl acrylate) on the hydrophilicity and binding tendency of common hemodialysis membranes: Molecular dynamics simulations and molecular docking studies. *J. Comput. Chem.* **2022**, *43*, 57–73. [[CrossRef](#)]
20. Mollahosseini, A.; Lee, K.M.; Abdelrasoul, A.; Doan, H.; Zhu, N. Innovative in situ investigations using synchrotron-based micro tomography and molecular dynamics simulation for fouling assessment in ceramic membranes for dairy and food industry. *Int. J. Appl. Ceram. Technol.* **2021**, *18*, 2143–2157. [[CrossRef](#)]
21. Mollahosseini, A.; Saadati, S.; Abdelrasoul, A. A Comparative Assessment of Human Serum Proteins Interactions with Hemodialysis Clinical Membranes using Molecular Dynamics Simulation. *Macromol. Theory Simul.* **2022**, *31*, 2200016. [[CrossRef](#)]
22. Mollahosseini, A.; Abdelrasoul, A. Molecular dynamics simulation for membrane separation and porous materials: A current state of art review. *J. Mol. Graph. Model.* **2021**, *107*, 107947. [[CrossRef](#)]
23. Mollahosseini, A.; Abdelrasoul, A. Novel insights in hemodialysis: Most Recent theories on the membrane hemocompatibility improvement. *Biomed. Eng. Adv.* **2022**, *3*, 100034. [[CrossRef](#)]
24. Dobson, C.M. Protein folding and disease: A view from the first Horizon Symposium. *Nat. Rev. Drug Discov.* **2003**, *2*, 154–160. [[CrossRef](#)]
25. Goto, Y.; Adachi, M.; Muta, H.; So, M. Salt-induced formations of partially folded intermediates and amyloid fibrils suggests a common underlying mechanism. *Biophys. Rev.* **2018**, *10*, 493–502. [[CrossRef](#)]
26. Ashkezari, A.Z.; Jolfaei, N.A.; Hekmatifar, M.; Toghraie, D.; Sabetvand, R.; Rostami, S. Calculation of the thermal conductivity of human serum albumin (HSA) with equilibrium/non-equilibrium molecular dynamics approaches. *Comput. Methods Programs Biomed.* **2020**, *188*, 105256. [[CrossRef](#)] [[PubMed](#)]
27. Goodship, T.H. Fibrinogen in hemodialysis: The worst of both worlds? *Kidney Int.* **2003**, *63*, 379–380. [[CrossRef](#)]
28. Cacciafesta, P.; Humphris, A.D.L.; Jandt, K.D.; Miles, M.J. Human plasma fibrinogen adsorption on ultraflat titanium oxide surfaces studied with atomic force microscopy. *Langmuir* **2000**, *16*, 8167–8175. [[CrossRef](#)]
29. Werner, C.; Maitz, M.; Sperling, C. Current strategies towards hemocompatible coatings. *J. Mater. Chem.* **2007**, *17*, 3376–3384. [[CrossRef](#)]
30. Bergström, J.; Lindholm, B. What are the causes and consequences of the chronic inflammatory state in chronic dialysis patients? In *Seminars in Dialysis*; Blackwell Science Inc.: Boston, MA, USA, 2000.
31. Goicoechea, M.; De Vinuesa, S.G.; Gomez-Campderá, F.; Aragoncillo, I.; Verdalles, U.; Mosse, A.; Luño, J. Serum fibrinogen levels are an independent predictor of mortality in patients with chronic kidney disease (CKD) stages 3 and 4: New strategies to prevent cardiovascular risk in chronic kidney disease. *Kidney Int.* **2008**, *74*, S67–S70. [[CrossRef](#)]

32. Yu, J.; Lin, T.; Huang, N.; Xia, X.; Li, J.; Qiu, Y.; Yang, X.; Mao, H.; Huang, F. Plasma fibrinogen and mortality in patients undergoing peritoneal dialysis: A prospective cohort study. *BMC Nephrol.* **2020**, *21*, 349. [[CrossRef](#)] [[PubMed](#)]
33. Botan, V.; Backus, E.H.; Pfister, R.; Moretto, A.; Crisma, M.; Toniolo, C.; Nguyen, P.H.; Stock, G.; Hamm, P. Energy transport in peptide helices. *Proc. Natl. Acad. Sci. USA* **2007**, *104*, 12749–12754. [[CrossRef](#)]
34. Yamato, T.; Wang, T.; Sugiura, W.; Lapr evote, O.; Katagiri, T. Computational Study on the Thermal Conductivity of a Protein. *J. Phys. Chem. B* **2022**, *126*, 3029–3036. [[CrossRef](#)]
35. Peng, H.; Dang, L.; Toghraie, D. Molecular dynamics simulation of thermal characteristics of globulin protein dissolved in dilute salt solutions using equilibrium and non-equilibrium methods. *J. Therm. Biol.* **2023**, *113*, 103505. [[CrossRef](#)]
36. Fang, Y.; Bokov, D.O.; Hachem, K.; Sabetvand, R.; Alsultany, F.H.; Suksatan, W.; Hekmatifar, M.; Toghraie, D. The computational investigation of thermal conductivity of 11S globulin protein for biological applications: Molecular dynamics simulation. *J. Mol. Liq.* **2022**, *346*, 118267. [[CrossRef](#)]
37. Zhang, L.; Bai, Z.; Ban, H.; Liu, L. Effects of the amino acid sequence on thermal conduction through  $\beta$ -sheet crystals of natural silk protein. *Phys. Chem. Chem. Phys.* **2015**, *17*, 29007–29013. [[CrossRef](#)] [[PubMed](#)]
38. Mayo, S.L.; Olafson, B.; Goddard, W. DREIDING: A generic force field for molecular simulations. *J. Phys. Chem.* **1990**, *94*, 8897–8909. [[CrossRef](#)]
39. Humphrey, W.; Dalke, A.; Schulten, K. VMD: Visual molecular dynamics. *J. Mol. Graph.* **1996**, *14*, 33–38. [[CrossRef](#)] [[PubMed](#)]
40. Hanwell, M.D.; Hanwell, M.D.; Curtis, D.E.; Lonie, D.C.; Vandermeersch, T.; Zurek, E.; Hutchison, G.R. Avogadro: An advanced semantic chemical editor, visualization, and analysis platform. *J. Cheminform.* **2012**, *4*, 1–17. [[CrossRef](#)] [[PubMed](#)]
41. Mart nez, L.; Andrade, R.; Birgin, E.G.; Mart nez, J.M. PACKMOL: A package for building initial configurations for molecular dynamics simulations. *J. Comput. Chem.* **2009**, *30*, 2157–2164. [[CrossRef](#)]
42. Wypych, G. *Handbook of Polymers*; Elsevier: Amsterdam, The Netherlands, 2016.
43. Mollahosseini, A.; Abdelrasoul, A. Zwitterionization of common hemodialysis membranes: Assessment of different immobilized structure impact on hydrophilicity and biocompatibility of poly aryl ether sulfone (PAES) and cellulose triacetate (CTA) hemodialysis membranes. *Struct. Chem.* **2022**, *33*, 1965–1982. [[CrossRef](#)]
44. Jolfaei, N.A.; Hekmatifar, M.; Piranfar, A.; Toghraie, D.; Sabetvand, R.; Rostami, S. Investigation of thermal properties of DNA structure with precise atomic arrangement via equilibrium and non-equilibrium molecular dynamics approaches. *Comput. Methods Programs Biomed.* **2020**, *185*, 105169. [[CrossRef](#)]
45. Ponder, E. The coefficient of thermal conductivity of blood and of various tissues. *J. Gen. Physiol.* **1962**, *45*, 545–551. [[CrossRef](#)]
46. Tekin, I.O.; Pocan, B.; Borazan, A.; Ucar, E.; Kuvandik, G.; Ilikhan, S.; Demircan, N.; Ozer, C.; Kadayifci, S. Positive correlation of CRP and fibrinogen levels as cardiovascular risk factors in early stage of continuous ambulatory peritoneal dialysis patients. *Ren. Fail.* **2008**, *30*, 219–225. [[CrossRef](#)]
47. Prinsen, B.H.; Rabelink, T.J.; Beutler, J.J.; Kaysen, G.A.; De Boer, J.; Boer, W.H.; Hagen, E.C.; Berger, R.; Velden, M.G.D.S.-V.D. Increased albumin and fibrinogen synthesis rate in patients with chronic renal failure. *Kidney Int.* **2003**, *64*, 1495–1504. [[CrossRef](#)] [[PubMed](#)]
48. Giordano, M.; DE Feo, P.; Lucidi, P.; Depascale, E.; Giordano, G.; Infantone, L.; Zoccolo, A.M.; Castellino, P. Increased albumin and fibrinogen synthesis in hemodialysis patients with normal nutritional status. *J. Am. Soc. Nephrol.* **2001**, *12*, 349–354. [[CrossRef](#)] [[PubMed](#)]
49. Zoccali, C.; Mallamaci, F.; Tripepi, G.; Cutrupi, S.; Parlongo, S.; Malatino, L.S.; Bonanno, G.; Rapisarda, F.A.; Fatuzzo, P.M.; Seminara, G.; et al. Fibrinogen, mortality and incident cardiovascular complications in end-stage renal failure. *J. Intern. Med.* **2003**, *254*, 132–139. [[CrossRef](#)] [[PubMed](#)]
50. Fumagall, G.; Panichi, V. Biocompatibility of the Dialysis System. In *Critical Care Nephrology*; Elsevier: Amsterdam, The Netherlands, 2019; pp. 918–922. e2.
51. Chidambaram, T.; Oren, Y.; Noel, M. Fouling of nanofiltration membranes by dyes during brine recovery from textile dye bath wastewater. *Chem. Eng. J.* **2015**, *262*, 156–168. [[CrossRef](#)]
52. Ma, B.; Wu, G.; Li, W.; Miao, R.; Li, X.; Wang, P. Roles of membrane–foulant and inter/intrafoulant species interaction forces in combined fouling of an ultrafiltration membrane. *Sci. Total Environ.* **2019**, *652*, 19–26. [[CrossRef](#)]
53. Khan, H.M.; He, T.; Fuglebakk, E.; Grauffel, C.; Yang, B.; Roberts, M.F.; Gershenson, A.; Reuter, N. A role for weak electrostatic interactions in peripheral membrane protein binding. *Biophys. J.* **2016**, *110*, 1367–1378. [[CrossRef](#)]
54. Zhao, J.; He, G.; Liu, G.; Pan, F.; Wu, H.; Jin, W.; Jiang, Z. Manipulation of interactions at membrane interfaces for energy and environmental applications. *Prog. Polym. Sci.* **2018**, *80*, 125–152. [[CrossRef](#)]
55. Harano, Y.; Yoshidome, T.; Kinoshita, M. Molecular mechanism of pressure denaturation of proteins. *J. Chem. Phys.* **2008**, *129*, 10B607. [[CrossRef](#)] [[PubMed](#)]
56. Durand, D.; Gimel, J.; Nicolai, T. Aggregation, gelation and phase separation of heat denatured globular proteins. *Phys. A Stat. Mech. Its Appl.* **2002**, *304*, 253–265. [[CrossRef](#)]
57. Rabe, M.; Verdes, D.; Seeger, S. Understanding protein adsorption phenomena at solid surfaces. *Adv. Colloid Interface Sci.* **2011**, *162*, 87–106. [[CrossRef](#)] [[PubMed](#)]

**Disclaimer/Publisher’s Note:** The statements, opinions and data contained in all publications are solely those of the individual author(s) and contributor(s) and not of MDPI and/or the editor(s). MDPI and/or the editor(s) disclaim responsibility for any injury to people or property resulting from any ideas, methods, instructions or products referred to in the content.